The Numerical Computation of Aircraft Response to Arbitrary Vertical Gust Distributions

Jiguang An*
The Chinese Aerodynamic Research and Development Center, Mianyang, China
Zhen Yan†
Shanghai Jiao Tong University, Shanghai, China
Chuanren Qiu‡
Shanghai Aircraft Company, Shanghai, China
and
Wenbo Zhou§
Shanghai Jiao Tong University, Shanghai, China

The partial results of a subsonic longitudinal response that has been used in some practical design work are summarized. The aircraft gust response consists of three modes: dynamic, control and elastic structure. In the control response mode, the responses of both the pilot and the gust alleviator have been considered. The type of gust may be either discrete or continuous with an arbitrary velocity distribution. The aircraft are also arbitrary and include conventional and canard configurations. The method of time history is the mainstay of this computing program. The disturbed flight path is divided into several thousand time intervals; during each interval, the aerodynamic, flight dynamic, structural elastic, and control equations are solved in succession. The resulting parameters are used as the input of the next interval. The method of finite elementary solutions is arranged to calculate the unsteady aerodynamic loadings over the wing and tail surfaces. A new parallelogrammic paneling is suggested to minimize the number of influence coefficients. Some comparisons of the results obtained here with those of analytical methods have been made and it is found that they agree quite well.

Nomenclature

a = speed of sound
A = aspect ratio
Δc = chordwise length of panel
C = chord length
C_L = lift coefficient
H = flight altitude
K = influence coefficient
$K(\Omega)$ = frequency response function
m = number of panels on a wing
M_0 = flight Mach number
N = number of interval
n = normal load factor with lift L and aircraft weight W, $(L/W)-1$
$S_g(\Omega)$ = spectral density of gust
$S_n(\Omega)$ = spectral density of n
t = time
T = number of gusts encountered per minute
Δt = time interval
U_0 = flight velocity, $=M_0 a$
V_g = vector of gust velocity $= U_g\hat{i}+V_g\hat{j}+W_g\hat{k}$
W_e = local normal velocity on wing due to elasticity
W_g = local normal velocity on wing
x,y,z, = body coordinates, Fig. 5
x_g,y_g,z_g = ground coordinates, x_g is aligned to initial flight velocity, z_g is vertical
α = angle of attack
α_g = angle between flight path and ground or flight path angle
Γ = strength of vortex ring
δ = deflection angle of control surface
ϵ_e = local angle of attack due to elasticity
λ = wave length
Λ = sweep angle of wing leading edge
ω_z = pitching angular velocity
$\Omega=2\pi/\lambda$ = reduced frequency

Superscripts

$(\ )^*$ = fundamental solution
$(\ )'$ = d/dt, the first derivative with respect to t
$(\ )''$ = d^2/dt^2, the second derivative with respect to t

Introduction

THE theoretical analysis of gust response plays an important role in modern aircraft design. For commercial aircraft, the progress made in gust response research means further decreases in structural weight and increases in safety. For military aircraft, especially low-altitude attack aircraft, gust response characteristics are one of the most important factors determining the riding properties and fire control capabilities.

Turbulent gusts, terrain gusts, wave gusts, and wind shears exist in the atmosphere; some are discrete and others are continuously distributed. Worldwide, meteorologists and aerodynamists have extensively studied these phenomena and their results have been summed up in air/worthiness regulations. Early in 1970, the Chinese Aerodynamic Research and Development Center (CARDC) undertook an extensive project called the "Computation and Analysis of Aircraft Gust

Presented as Paper 84-2075 at the AIAA Atmospheric Flight Mechanics Conference, Seattle, WA, Aug. 21-23, 1984; received Oct. 31, 1984; revision submitted April 22, 1985.

*Senior Engineer (presently, Visiting Professor, Shanghai Jiao Tong University).
†Professor.
‡Engineer.
§Lecturer.

Response'' aimed at formulating a complete numerical computer program. Some parts of this project were investigated by the Department of Engineering Mechanics of Shanghai Jiao Tong University. This paper summarizes the subsonic longitudinal part of the project.

Basic Concepts

When an aircraft in horizontal steady flight encounters gusts, the primary disturbances are caused by the gust velocity; subsequently, secondary disturbances come from the dynamic, control, and elastic structural responses of the aircraft itself. Also, as the flight path deviates from the horizontal, the wind variation with altitude (wind shear) and even the power spectrum of the continuous gusts must be considered. Dynamic response refers to the rotating and heaving motions caused by aerodynamic force variations. Control responses are those surface deflections that are the reactions of a pilot, autopilot, or gust alleviator to the disturbances. The dynamic and static deflections produced by aerodynamic loadings are called the structural elastic response. The unsteady aerodynamic time-lagging effects of the disturbed airplane also induce perturbance of the local angle of attack.

In dealing with such a complicated state of affairs, it would seem impossible to adopt any numerical method with a more analytical treatment, even though it could greatly reduce the calculating work. The method of time history (MTH) has been selected as the basis of treating this problem. The aerodynamic calculation is done by the method of finite elementary solutions (MFES). In order to reduce the amount of calculation, research about computing techniques was done and it was found that the computation of the entire gust response could be accomplished on a medium-sized computer.

With the time history method, the gust encounter process is divided into many time intervals having the same value Δt; the computations are then done at all instants in sequence until the end of entire process. Normally, the time interval will be chosen as $1\times10^{-3}-10^{-2}$ s. For a discrete gust, the computed encounter process is about 30 s, but may be increased to 2 min for a continuous gust. In this way, the number of computing instants varies between 3000 and 100,000.

Figure 1 shows the flow diagram of an instant calculation cycle of an aircraft's gust response. At every instant, the known data needed (such as pitching angular velocity ω_z, time rate of change in the angle of attack α', control surface deflection δ, local angle of attack ϵ_e, and normal velocity W_e induced by structural elasticity, etc.) are collected from the computation results of the previous instants. Gust velocities V_g distributed along the airplane surface are given, but may vary with flight altitude H. On the basis of these aerodynamic state parameters, the MFES calculations of unsteady and steady areodynamics are made to solve the areodynamic loads acting on the aircraft. Through proper integration or summation, we obtain the aerodynamic forces and moments at that instant and then substitute these into the flight dynamics equations to get the pitching angular acceleration $\dot{\omega}_z$ and α'' (the second derivative of α with respect to t). Through time integrations, ω_z and α' for the next instant are found. On the other hand, parameters such as the flight path angle α_g and the load factor n are fed into the control equations to find the time rate of change in the deflection angle of the control surface δ'. The parameters have the deflection angle of control surface δ for next instant after an operation of time integration in the period Δt. Altitude H is fed into the original gust distribution model to supply gust velocity distributions V_g for the next instant. At the same time, the ground coordinates of the aircraft have been stored, which will be linked up to form flight path as soon as the entire process is completed.

During computation of the unsteady aerodynamics, one must account for the time lag effects of all previous instants together with those aerodynamic state parameters at the present instant; in other words, the instantaneous aerodynamic characteristics of an aircraft are determined by both the state parameters at this instant and the vortex wake influences of all the previous instants. Because the unsteady computations are very difficult and complicated, we are forced to simplify the mathematical model of the whole aircraft; for example, the wings and tail are approximated as thin planes and only the first-order of the wing/body interference is considered. The distortions of the vortex wake are neglected. Then we have to arrange some steady-state computations with a more practical model, even using some wind tunnel tests to correct the unsteady results. The steady computations are conducted individually on both accurate and rough (used in unsteady computations) models. Then we use a proportional factor between these results to correct unsteady aerodynamic characteristics, as shown in Fig. 2.

In fact, with a given aircraft configuration, flight Mach number, and gust distribution, the so-called "fundamental solutions" should be calculated beforehand and the results stored. During the MTH process, unsteady forces at each instant can be regarded as the linear addition of these fundamental solutions that individually emerged from all the

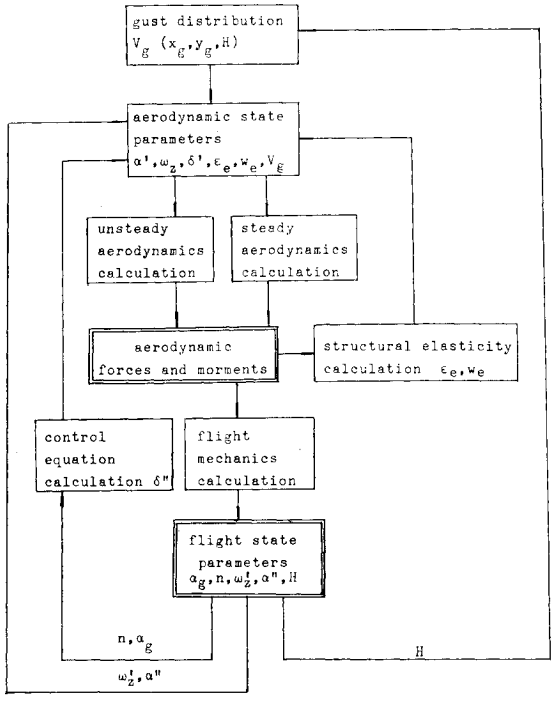

Fig. 1 Flow diagram for computating the gust response of an aircraft.

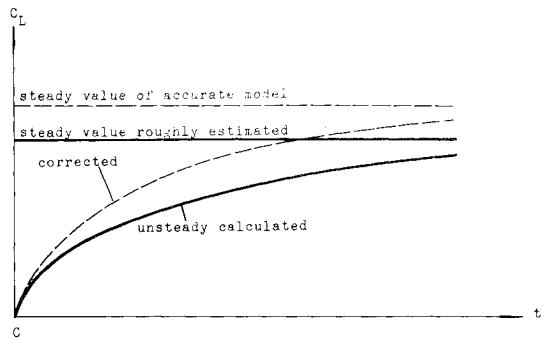

Fig. 2 Correction of calculated unsteady results with regard to steady results.

former instants. This is the numerical form of Duhammel integration, as shown in Fig. 3. For example, the unsteady lift coefficient induced by α' at instant t can be written as

$$C_L(t) = \sum_{t_k=t_1}^{t} [\alpha'(t_k)\Delta t] C_L^*(t-t_k) \tag{1}$$

where C_L^* is the fundamental solution for the lift coefficient of heaving.

There are five unsteady fundamental solutions, namely:

1) Heaving, refers to $\alpha' = 1$.
2) Pure rotation, refers to $\omega_z = 1$.
3) Deflection of control surface, refers to $\delta' = 1$.
4) Gust, refers to $W_g = 1$.
5) Structural elasticity, including bending and torsion of the first and second orders.

Unsteady Aerodynamic Calculation

The unsteady motions and aerodynamic forces are of two types: oscillating and transient. The time variable has little effect on the computation of the former. The problem can be solved by oscillating doublet lattices in the same way as steady problems. But in the more complicated transient case, we must consider the whole history of vortex shedding and here the MTH shows its potential.

References 1-3 studied the numerical computation of an unsteady subsonic wing, which shed vortex rings one by one from the trailing edge; these free vortex rings were allowed to distort. In Reference 4, this method was used to investigate the distortion of the vortex wake shape and its effects on the tail surface. Djojodihardjo and Widnall[5] treated the unsteady problems of a three-dimensional wing with thickness and wake distortion, but the problems were limited to incompressible flows. Belochelkovski and Kolesnikov[6] developed the MFES method, in which the vortex rings would be elongated as time went by. However, it apparently could not be extended to a case with wake distortion. Figure 4 shows the differences between the vortex rings used in Ref. 6 and this paper.

The value Δt selected as the time interval should be matched with lattice length ΔC, $\Delta t = \Delta C/U_0$, so that the wing vortex ring distribution at a certain instant t_1 will move downstream a distance of one lattice length at the next instant $t_2 = t_1 + 1$. In order to satisfy the boundary conditions on the wing surface, a new set of vortex rings appears at instant t_2, as shown in Fig. 5. At each instant t, in solving the strength of these newly born vortex rings, the normal velocities induced by all of the former vortex sets on the wing control points must be taken account on the right-hand side of the boundary equations. The boundary equations at instant t may be written as

$$K_{i-j}^t\{\Gamma_i^t\} = \left\{W_j^t + \sum_{t_k=t_1}^{t-1} \sum_{i=1}^{m_{tk}} K_{i-j}^t \Gamma_i^{tk}\right\} \tag{2}$$

where K_{i-j}^t is the normal influence coefficient of the ith vortex ring to the jth control point at instant t, Γ_i^t the strength of the ith vortex ring at this instant, and W_j^t the normal velocity produced by the gust, dynamic, control, and elastic responses at this instant. The last term with two summations counts the normal velocities induced by all the free vortex rings generated from the previous instants. m_{tk} is the number of vortex rings that affect the control point j at instant t_k. Details of computing scheme and formulas are published in the first part of Ref. 7.

In order to bring about a large-scale reduction in the amount of computation, the panel shapes of the lifting surfaces should be the same—at least, the chordwise panels at the same spanwise location should have the same shape. In our early program, rectangular panels were employed (Fig. 6a), resulting in saw-toothed leading and trailing edges. Therefore, serious jumping errors appeared in the calculated load distribution. Belochelkovski[6] adopted parallelogram panels (Fig. 6b) with the swept sides parallel to the trailing edge, but the leading edge was still saw-tooth. Especially for a delta wing, the panels became rectangular. According to Ref. 8, our parallelogrammic panels are parallel to the leading edge (Fig. 6c) and the control points of the trailing-edge panels shift a certain distance forward rather than remaining at the original position of panel centroid.

The speed of sound is infinite in incompressible flow, so entire vortex rings, no matter when they are generated, will affect any control point j instantaneously. Then, in Eq. (2), $m_{tk} = m$, m is the number of panels on a wing and the influence coefficient matrix K_{i-j}^t is full. On the other hand, in compressible flow only, some vortex rings generated at instant t_k and propagated to point j after a time interval $(t-t_k)$ are influencial. Therefore, the method raises a problem of judgment to determine which vortex rings have affected con-

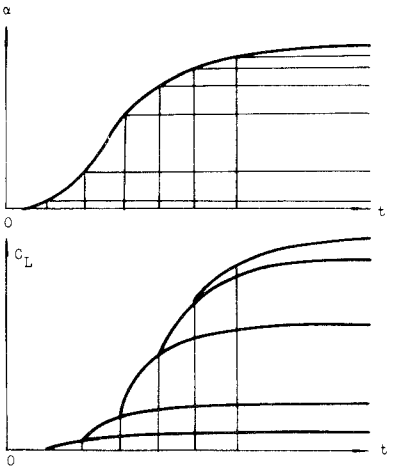

Fig. 3 Numerical form of Duhammel's integration.

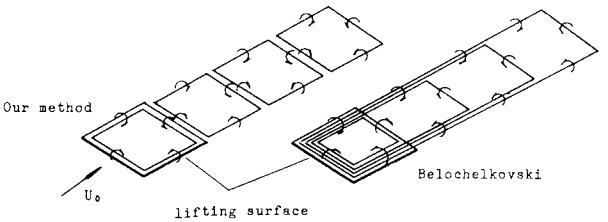

Fig. 4 Elementary solutions used in this paper and by Belochelkovski.[6]

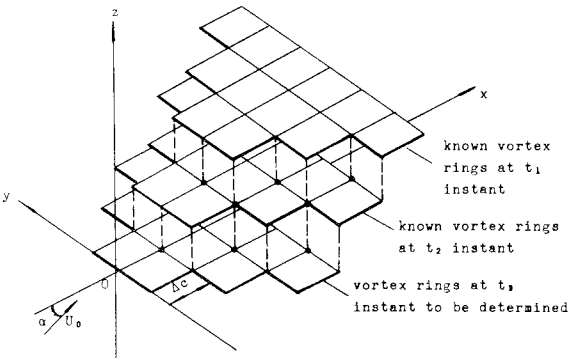

Fig. 5 Vortex ring arrangement of a triangular wing at t_3 instant.

trol point j. Because the vortex rings used in this method are different from those in Ref. 6, the judgment will also be different.

In MTH, we assume that all the perturbance generated in time interval between instant (t-1) and t are lumped at the latter instant t. These effective vortex rings generated at instant t are bounded in a circle with radius $\alpha\Delta t$ (Fig. 7) and those at instant (t-1) are bounded between circles with radii $a\Delta t$, $2a\Delta t$, etc. The longitudinal distance between the centers of two neighboring circles is $U_0\Delta t=\Delta C$. The so-called effective vortex rings consist of a newly born vortex and those born earlier at this position that have moved downstream. When calculating the influence coefficients, it is necessary to add $U_0(t-t_k)$ to the value of x.

Under this condition, a panel may be divided into several areas that become effective at different instants. The ith panel in Fig. 7 is divided into three areas in Fig. 8 and its vortex ring becomes three smaller vortex rings with the same strength, which belong to three instants $(t-1)$, $(t-2)$, and $(t-3)$, respectively.

The influential effect of a vortex ring is equal to the uniformly distributed normal doublets inside the ring, so that the influence of any vortex ring with irregular shape is really the surface integration of doublets.[6,7] In practice, the curvilinear sections of a vortex ring may be approximately replaced by straight lines in order to apply Biot-Savart law directly. Our experience shows that panels may not be broken down except those near control point j. If the centroid of a panel locates in the effective region of certain instant, then the whole panel vortex ring may be considered as belonging to that instant. For example, the whole vortex ring in Fig. 8 can be regarded as that belonging to instant $(t-2)$. Therefore, the computation time is decreased significantly.

Reference 5 and 6 suggested that the vortex segments of the last row on trailing edge should shift a small distance downstream in order to satisfy the Kutta condition as soon as the unsteady motion starts. But in this program, these trailing-edge vortices remain there, because the physical mechanism of the start of the flowfield is still in doubt; by intuition, it seems that all of the free vortices must be produced and released by the wing itself.

In early papers such as Refs. 9 and 10, there was a starting lift arising from aerodynamic inertia. In using MFES, this starting lift has been automatically included, as shown in Ref. 1. As in the calculation of the heaving motion, the unsteady lift at instant $t=c/\Delta C$ (the starting vortex has already traveled one chord length) has the same value as that obtained from aerodynamic inertia. Therefore, if we shift the starting instant to $t=c/\Delta C$, the calculated results will coincide with those from analytical methods.

The computation of any unsteady fundamental solution is made only to the instant when the vortex wake has shed about six chord lengths downstream. Then the unsteady aerodynamic curve is prolonged to approach the steady value according to an exponential curve.

For a complete aircraft, the wing and horizontal tail are calculated simultaneously and the unsteady downwash interference induced by the wing on the tail must be smoothed by a special program; otherwise, singularities will appear.

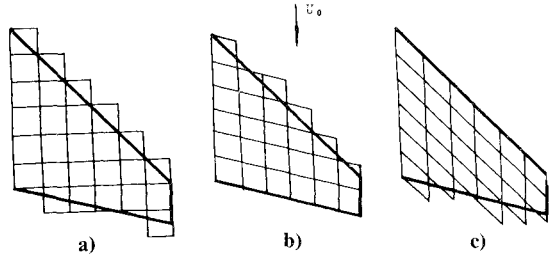

Fig. 6 Three forms of wing lattice: a) rectangular; b) parallel to trailing edge of wing[6]; c) parallel to leading edge of wing.[7,8]

Applications

The results of applying this technique to an isolated wing have proved that MFES is an efficient tool for computing unsteady aerodynamic loads. Figure 9 shows the lift coefficient of a thin, two-dimensional wing when the wing enters a step gust and Fig. 10 the results for three elliptical planform wings with different aspect ratios. Both of Figs. 9 and 10 coincide with analytical results.

Some complete computations have been made for several aircraft encountering both discrete and continuous gusts. The gust response properties of an aircraft with aspect ratio $A=3.5$ and leading-edge sweep angle $\Lambda=40$ deg are given in Figs. 11-13. The time history of load factor n during flight through one cosine and ramp types of discrete gusts is shown in Fig. 11.

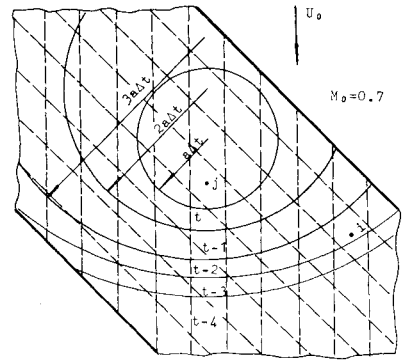

Fig. 7 Panels of former instants that influenced the control j at t instant.

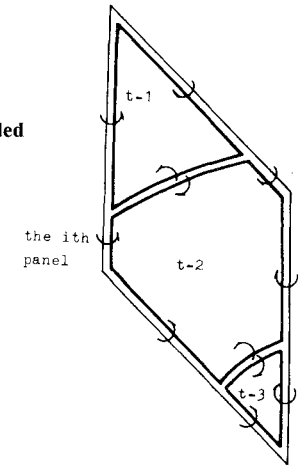

Fig. 8 ith panel of Fig. 7 divided into three instantaneous vortex rings.

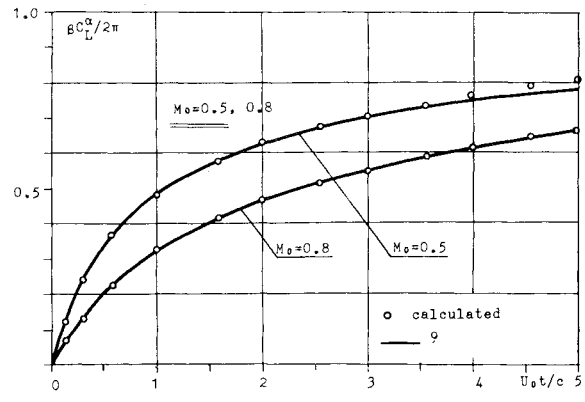

Fig. 9 Lift variation of two-dimensional plane wing encountering a step gust: comparison of calculation and analytical solution.[9]

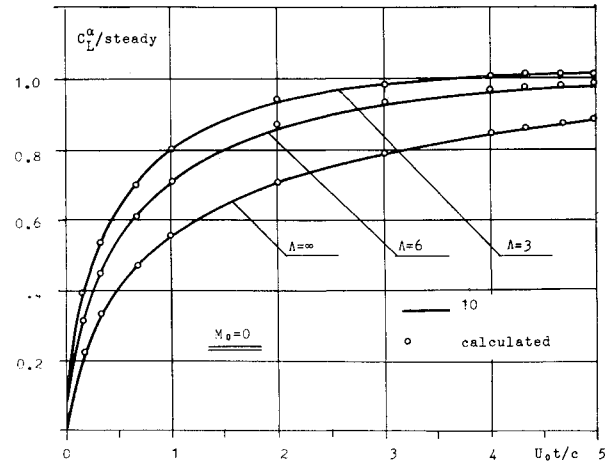

Fig. 10 Lift variation of wings of elliptical planforms encountering a step gust: comparison of calculations and analytical solutions.[10]

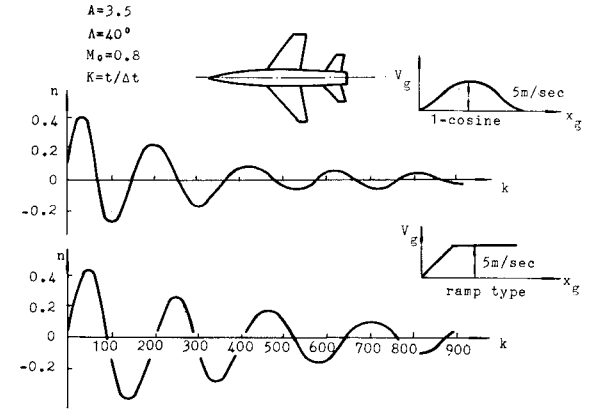

Fig. 11 Variation of load factor n with time of a typical aircraft when encountering discrete gust $\Delta t = 1/300$ s.

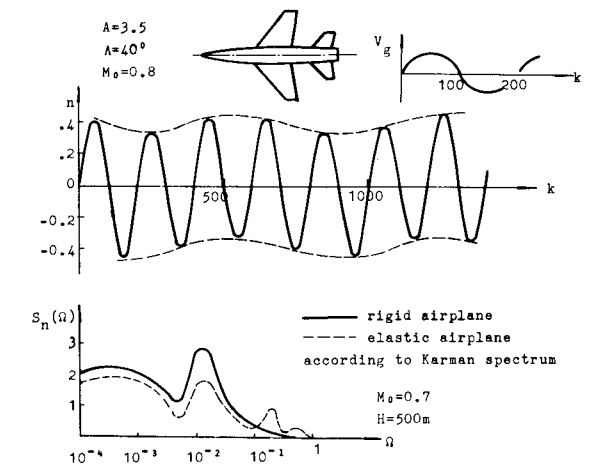

Fig. 12 Variations of n of former aircraft during flight through oscillating gust (top) and its load factor response spectrum (bottom).

The response properties of an aircraft flying through a continuous gust can be represented by its response spectrum $S_n(\Omega)$ as

$$S_n(\Omega) = |K(\Omega)|^2 S_g(\Omega) \tag{3}$$

where $S_g(\Omega)$ is a given spectrum of atmospheric turbulence and $K(\Omega)$ the frequency response function of the aircraft to be computed. In the third part of Ref. 7, the gust spectrum was divided into 20-50 frequency bands and the aircraft responses were computed according to unit sinusoidal gusts with each of those frequencies. The maximum value of load factor is $K(\Omega)$. The upper part of Fig. 12 shows a typical variation of load factor n during a flight through an oscillating gust and the lower part the response spectrum of both rigid and elastic aircraft. Figure 13 shows the relationship between load factor n and the number of gusts encountered per minute T.

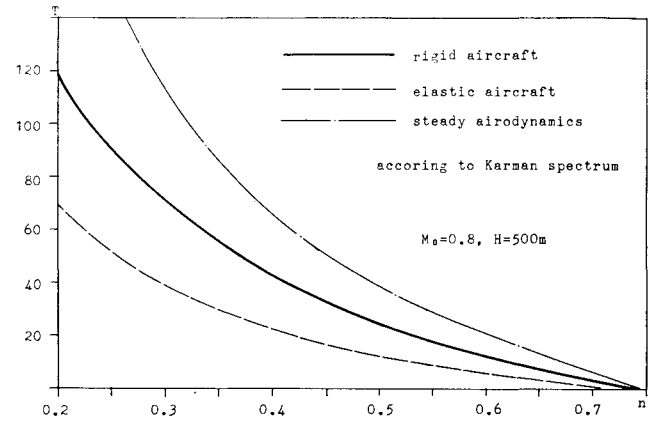

Fig. 13 Relationship of load factor n and number of gusts encountered per minute T of a former aircraft.

Our experience has proved that this computing method is quite effective and economical. When it is used on other problems such as aircraft maneuverability and response to wing sweep angle ariation (on variable sweep wing), the results are also satisfactory.

References

[1]An, J. "The Starting Problem and Wake Calculation of Two- and Three-Dimensional Thin Wings," Unpublished paper, CARDC, Mianyang, China, May 1971.

[2]An, J. "The Computation of Subsonic Unsteady Three Dimensional Thin Wings Using MFES," Unpublished paper, CARDC, Mianyang, China, April 1972.

[3]An, J., "The MFES is Subsonic Aerodynamics," CARDC, Mianyang, China, *Aerodynamic Research & Development*, No. 7, May 1977.

[4]Cheng, Z., "The Computations of Wing Wake Shapes and Tail Aerodynamic Characteristics," Unpublished paper, CARDC, Mianyang, China, June, 1974.

[5]Djojodihardjo, R. H. and Widnall, S. E., "A Numerical Method for the Calculation Linear, Unsteady Lifting Potential Flow Problems," *AIAA Journal*, Vol. 7, Oct. 1969, pp. 2001.

[6]Belochelkovski, C. M. and Kolesnikov, G. A., "The Calculation of Complex Planform Wings during Impulsive Starting with Subsonic Speeds," *Mechanics of Fluids and Gases*, No. 5 USSR Academy of Science, 1969, p. 129.

[7]An, J., Yan, Z., Qiu, C., and Zhou, W., "Gust Response Computation of Subsonic Aircraft: Part I—The Numerical Calculation of Subsonic Unsteady Airflow; Part II—A Synthetical Computing Method for Aircraft Response; Part III—The Spectrum Analysis of Aircraft Response due to Atmospheric Turbulence; Part IV—Computer Program and User's Guide," Dept. of Engineering Mech., Shanghai Jiao Tong University, Shanghai, China, March 1982.

[8]Ren, B., "A Basic Study to the Calculation of Unsteady Lifting Surfaces with Parallelogramic Panelling," Master Thesis, Shanghai Jiao Tong University, Shanghai, China, Oct. 1980.

[9]Lomax, H., "Lift Developed on Unrestrained Rectangular Wings Entering Gusts at Subsonic and Supersubsonic Speeds," NASA TN 2925, April 1953.

[10]Jones, R. T., "The Unsteady Lift of a Wing of Finite Aspect Ratio," NACA TR 681, 1940.